NeuroImage 79 (2013) 1–9

Contents lists available at SciVerse ScienceDirect

NeuroImage

journal homepage: www.eh.ovier.com/locate/ynimg

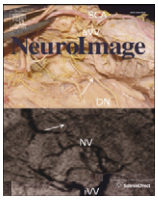

Selectivity for large nonmanipulab0/GS0(objlecse)-2695(ine)-285.4scene-sSelectiey

Introduction

The functional organization of object representations in the human visual cortex, especially the ventral temporal cortex (VTC), has been the focus of much recent research. Functional neuroimaging studies have provided evidence that different object domains evoke distinct responses in VTC. For example, specific regions of VTC respond selectively to particular object categories, such as faces, bodies, words, or places (Bracci et al., 2010; Chao et al., 1999; Cohen and Dehaene, 2004; Downing et al., 2001, 2006; Epstein and Kanwisher, 1998; Kanwisher, 2010; Kanwisher et al., 1997; Peelen and Downing, 2005).

A particularly strong type of categorical selectivity is observed with scene stimuli. Compared to pictures of faces, common objects or scrambled pictures, pictures of scenes or places elicit stronger activation in a region in the parahippocampal gyrus (the parahippocampal place area, PPA), along with two additional regions in the retrosplenial complex (RSC) and the transverse occipital sulcus (TOS) (e.g., Epstein and Kanwisher, 1998; Goh et al., 2004). These findings motivated hypotheses about the function of PPA, including that it processes peripheral visual information, certain geometrical features about openness or closeness, or spatial properties (e.g., Kravitz et al., 2011; Levy et al., 2001; Park et al., 2011; Ross and Oliva, 2010). Interestingly, a series of recent studies showed that PPA activity is also modulated by the type of objects, preferring objects that are part of a scene (e.g., buildings, Maguire et al., 2001), large (Konkle and Oliva, 2012; Mullally and Maguire, 2011; Troiano et al., in press), with strong contextual associations (e.g., Bar and Aminoff, 2003), or those that more easily evoke a sense of space or place (Mullally and Maguire, 2011).

The degree to which visual object properties underlie the observed object categorical effects in PPA remains debated. One type of proposal is that the preference for scenes and some types of objects is driven by its sensitivity to certain visual aspects that are shared between scenes and these objects, e.g., peripheral visual information being more important (e.g., Konkle and Oliva, 2012). Alternatively, it might be because these regions are at least partly engaged in the more abstract interpretation of the stimulus, and the selectivity reflects how strongly the objects imply a scene/place and information useful for spatial navigation (e.g., Troiano et al., in press). In the

---

* Corresponding author at: State Key Laboratory of Cognitive Neuroscience and Learning, Beijing Normal University, Beijing 100875, PR China. Fax: + 86 10 5880 2911.

E-mail address: ybi@bnu.edu.cn (Y. Bi).

1053-8119/$ – see front matter
http://dx.doi.org/10.1016/j.neuroimage.2013.04.051

present study we tested congenitally blind participants to investigate whether knowledge of visual object properties is required for object

In the experiment the participants viewed the object photographs through a mirror attached to the head coil adjusted to allow foveal viewing of a back-projected monitor (refresh rate: 60 Hz; spatial resolution: 1024 × 768). The pictures were presented sequentially (666 ms; ISI = 0) in blocks of 30 items, all from the same category. Each block lasted approximately 20 s, followed by 20 s of fixation. The blocks were repeated four times in the experiment. The order of items within a block was constant across the participants, as was the order of the blocks. Consecutive blocks were never from the same category. This single-run task lasted 8 min and 10 s.

Experiment 3 — Scene localizer

We carried out a separate scene localizer experiment on the sighted participants who participated in the previous two experiments, and we were able to recruit back four participants. We selected black-and-white pictures of 30 scenes (300 ∗ 300 pixels) and 30 objects (10 cars, 10 flowers and 10 chairs, 400 ∗ 400 pixels). The stimuli were presented in 16 s blocks, separated by 10 s of fixation. Each block had 16 pictures, all from the same condition (each picture was presented for 800 ms, ISI = 200 ms). Scene and object blocks were presented in alternating fashion, with eight blocks of each condition occurring in one run of 7 min and 16 s long. The participants pressed a button with the left index finger rapidly whenever they saw two consecutive identical pictures. Each block and each category had an equal chance of having 0, 1, or 2 identical picture pairs.

MRI data acquisition

Structural and functional MRI data were collected with a 3 T Siemens Trio Tim scanner at the BNU MRI center. A high-resolution 3D structural data set was acquired with a 3D-MPRAGE sequence in the sagittal plane (TR: 2530 ms, TE: 3.39 ms, flip angle: 7°, matrix size: 256 × 256, 144 slices, voxel size: 1.33 × 1 × 1.33 mm, acquisition time: 8.07 min). BOLD signals were measured with an EPI sequence (TR: 2000 ms, TE: 30 ms, flip angle: 90°, matrix size: 64 × 64, voxel size: 3.125 × 3.125 × 4 mm, inter-slice distance: 4.6 mm, number of slices: 33; slice orientation: axial).

The scanning procedure for the blind group used the following order: a functional resting-state run for 6 min and 40 s; a 3D structural scan; the size judgment experiment. The sighted group underwent the same scan procedure as that for the blind participants except that ten participants did not receive the resting-state run. Furthermore, all sighted participants subsequently performed the passive picture viewing experiment at the end of the session. In the resting-state run, the participants were asked to lie still and not to think of anything in particular. In both the resting-state run and the auditory task runs the sighted participants were asked to keep their eyes closed. The scene localizer was carried out in another session more than three weeks later, which included one scene localizer run and a 3D structural scan. E-prime 1.1 (Schneider et al., 2002) was used for controlling stimulus presentation and recording responses.

fMRI data analysis

fMRI data were analyzed using BrainVoyager QX v2.3. The first 28 s in each run of the auditory size judgment task (the practice block) and 10 s in that of the passive picture-viewing task (fixation) were discarded. Preprocessing of the functional data included 3D motion correction with respect to the first (remaining) volume of the run scanned closest to the 3D structural data for each experiment, spatial smoothing (Gaussian filter, 6-mm Full Width Half Maximum), and temporal filtering (high-pass (GLM-Fourier): 3 sines/cosines for the one-back picture viewing experiment and 1 sines/cosines for other experiments). For each participant, functional data were then registered to her/his anatomical data. Finally, functional and anatomical volumes were transformed into a standardized space (Talairach and Tournoux, 1988), and functional data were resampled to 3 × 3 × 3 mm resolution.

All functional data were then analyzed using the general linear model (GLM). We included three predictors of interest corresponding to the three categorical conditions and six motion parameters as predictors of no interest.

We first carried out a whole-brain conjunction analysis for regions showing selectivity for large nonmanipulable objects: random-effect GLM analyses for large nonmanipulable objects > animals and large nonmanipulable objects > tools, each at the threshold of $p < .01$ uncorrected, cluster size > 7 resampled voxels, 189 mm^3, resulting in a conjunction threshold of $p < .001$ uncorrected. The cluster-level estimation for each contrast is adopted from the cluster-level statistical threshold estimator of BrainVoyager, based on the map's spatial smoothness and on an iterative procedure (Monte Carlo simulation with 1000 iterations). To quantify the relationship between the regions showing large nonmanipulable object selectivity and scene preference, we further carried out region-of-interest (ROI) analyses, defining ROIs using the full activation on the group level at $p < .05$ Bonferroni corrected, fixed effect and then carried out analyses using mean beta-values of different conditions for independent data sets in each ROI.

The functional connectivity of the resting-state data was analyzed using Statistical Parametric Mapping (SPM8, http://www.fil.ion.ucl.ac.uk/spm), the Resting-State fMRI Data Analysis Toolkit (REST, Song et al., 2011, http://www.restfmri.net) and Data Processing Assistant for Resting-State fMRI (DPARSF) (Yan and Zang, 2010). The first 10 volumes of the resting-state run of each participant were discarded for signal equilibrium and adaptation of the participants to the scanning noise. Next, slice timing and head motion correction were performed. A mean functional image was obtained for each participant, which was subsequently normalized to the EPI template. After the linear trend of the time courses was removed, a band-pass filter (0.01–0.08 Hz) was applied to reduce low-frequency drift and high-frequency noise. Finally, spatial smoothing (4-mm FWHM Gaussian kernel) was conducted to decrease spatial noise.

The functional connectivity was calculated by correlating the time series of each voxel with the seed region defined by the whole-brain contrasts. The seed region was obtained by creating a sphere with 6 mm radius around the peak seed voxel. Then, Fisher z-score transformations were conducted for the correlation coefficients to generate a z-FC map for each participant. To identify the regions showing significant functional connectivity with the seed(s), we did one sample t-tests on these individual z-FC maps to see whether they were significantly different from zero ($p < .05$, AlphaSim corrected). Only the regions showing positive correlations were presented.

The functional connectivity analyses were conducted on the gray matter mask generated using the following procedure. We included the voxels with a probability higher than 0.4 in the SPM5 template onto the gray matter mask. Given the signal distortion in cerebellum, we also excluded the cerebellar regions (#91–#116) in the Automated Anatomical Labeling (AAL) template (Tzourio-Mazoyer et al., 2002). In total, there were 36,272 voxels in the gray matter mask.

Results

Behavioral results

For the auditory size judgment experiment, the blind and t funct25.h33.4(-0

fMRI results

We have organized the fMRI results as follows: First we present whole-brain results for selectivity to large nonmanipulable objects using conjunction analyses of large nonmanipulable object > tool and large nonmanipulable > animal; We then compare the observed regions with regions defined in the sighted scene localizer task; Finally we show the resting-state functional connectivity patterns of the PPA region with the large nonmanipulable object selectivity. The overall task effects (all conditions versus baseline) in both participant groups (blind and sighted) are presented in the Supplementary material (Supplementary Results and Supplementary Fig. 1).

Whole-brain analyses testing for selectivity to large nonmanipulable objects

We first computed whole-brain (random effects) conjunction analyses of large nonmanipulable object > tool and large nonmanipulable > animal using the same threshold ($p < .01$ uncorrected, cluster size > 7 resampled voxels, 189 mm^3) in all experiments (Fig. 1a). In the sighted participants' picture viewing experiment, a bilateral medial VTC region close to PPA showed highly significant selectivity for large nonmanipulable objects. Bilateral transverse occipital sulcus (TOS) also showed large nonmanipulable object selectivity. Similar trends in bilateral retrosplenial complex (RSC) were observed without the cluster size threshold (i.e., $p < .01$ uncorrected). In the sighted participants' auditory experiment, bilateral PPA, bilateral RSC and left TOS showed selectivity fyc0> 7drge (a27.9(n)20.7(m)0(a)31.9(n)0(i)34.2(pu)1.8(u)0(l8(l)13.6(-)9.2(r)17.2(j)13.

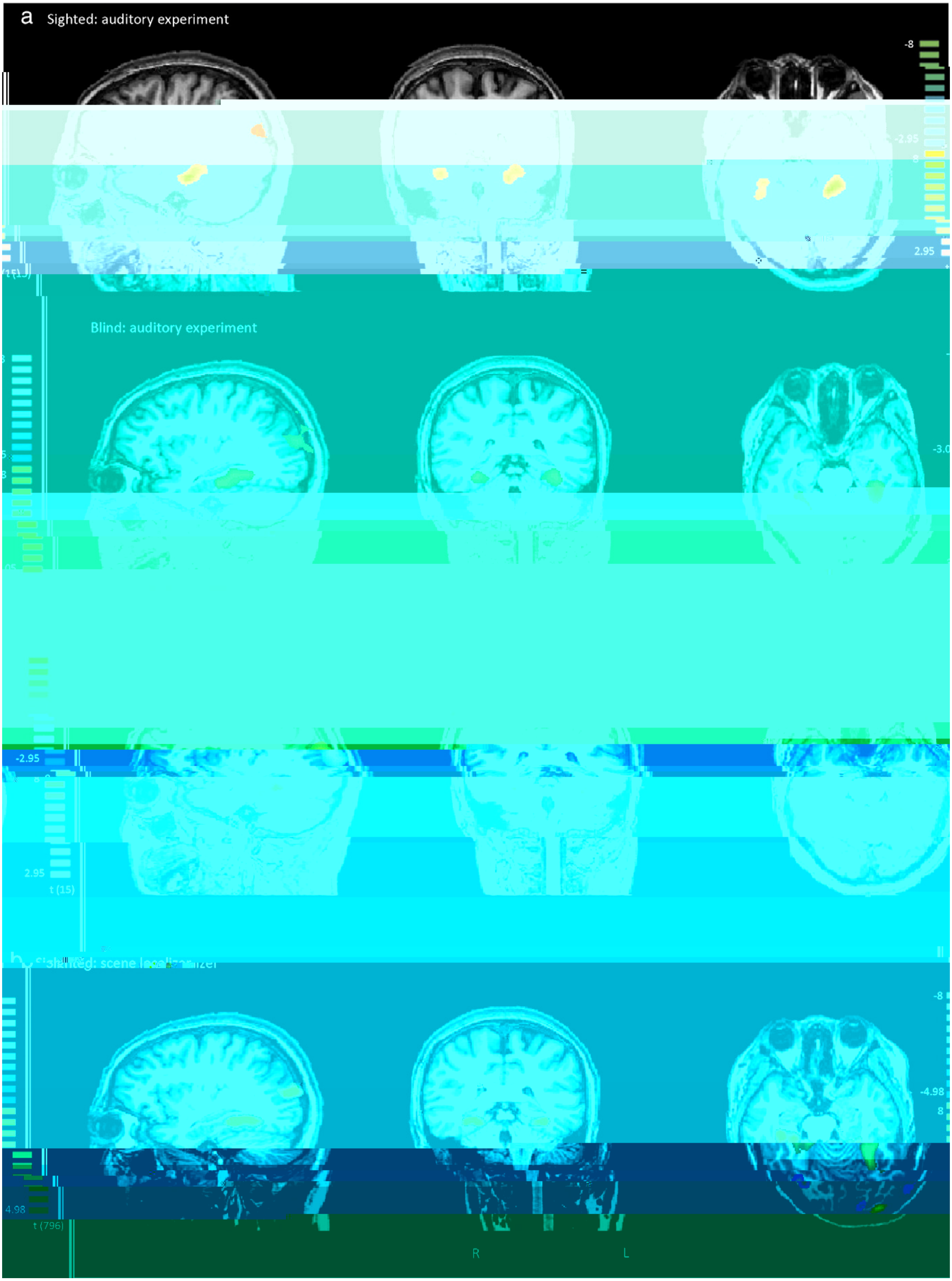
a
Sighted: auditory experiment
-8
-2.95
8
2.95
t (15)
Blind: auditory experiment
-3.0
-2.95
2.95
t (15)
b
Sighted: scene localizer
-8
-4.98
8
4.98
t (796)
R
L

but it was marginally significant in right ROI ($t\ (15) = 1.9$, $p = .07$) with higher response to animals than to tools (Figs. 2c–d).

Intrinsic functional connectivity patterns of the regions showing large nonmanipulable object selectivity

We explored the intrinsic functional connectivity patterns of regions showing category specificity for large nonmanipulable objects. We used the observed peak coordinates in PPA obtained in the above conjunction analyses (large nonmanipulable object > tool and large nonmanipulable object > animal, for sighted auditory experiment and blind auditory experiment), and calculated the correlation between the time series of the seed regions and all other voxels in the brain from the resting-state data. For the sighted participants (seven individuals), the left PPA ROI was found to be significantly connected with the right PPA, bilateral RSC, left anterior temporal lobe, and bilateral medial frontal gyrus. The right PPA ROI was significantly connected with the left PPA, right TOS, bilateral RSC, right anterior temporal lobe, and right medial frontal gyrus (Fig. 3; $p < .05$ AlphaSim corrected). For the blind group, we observed that the left PPA ROI showed significant functional connectivity with the right PPA, right TOS, bilateral RSC, right anterior temporal lobe, bilateral medial frontal gyrus, and right superior temporal gyrus. The right PPA ROI showed significant functional connectivity with the left PPA, bilateral TOS, bilateral RSC, right fusiform gyrus, right middle frontal gyrus, and bilateral anterior temporal lobe (Fig. 3; $p < .05$ AlphaSim corrected).

Discussion

In the present study, we explored the pattern of object selectivity in PPA in congenitally blind participants and sighted participants using an auditory object size jup5(u,)-32 objects in the current study. In additional analyses, we replicated this finding (see Supplementary material). When taking this “inanimate” region as ROI, we found that in both blind (auditory experiment) and sighted groups (picture viewing experiment), large nonmanipulable objects evoked significantly higher BOLD responses compared to the other two categories, while there was no difference between the activation to tools and animals (Supplementary material). These additional results thus suggest a re-interpretation of the inanimate preference reported previously (Mahon et al., 2009), showing that selectivity was specifically driven by the large nonmanipulable objects rather than by inanimate objects more generally.

A further interesting data point regarding the animacy effect was observed in this analysis: Animals evoked significantly higher activation in the bilateral occipital temporal cortex and the right fusiform gyrus compared to tools and large nonmanipulable objects in the sighted group's picture viewing experiment. However, when using these brain regions as ROIs, we did not find any difference between response to animals and to other two categories in both groups' auditory experiments (Supplementary material and Supplementary Fig. 3). This finding differed somewhat from Mahon et al. (2009), who reported a small cluster in left lateral occipital cortex in which similar animate > inanimate effects were observed in the sighted group performing visual and auditory tasks, and the blind participants performing auditory experiments. Note, however, that those results were observed using fixed effect analyses at a lenient statistical threshold ($p < .05$, uncorrected for multiple comparisons). It is possible that their observations may not generalize to other participants. Our finding of weak (or even absent) animal selectivity in the auditory experiment in both sighted and blind participants contrasts with the input-independent large nonmanipulable artifact selectivity, and suggests an interesting interaction between object domains and input modalities, at least in the sighted participants. Selectivity for animals has previously been shown to be modality-specific. The effects were rarely present when the stimuli were written or auditory words instead of pictures (Devlin et al., 2005; Price et al., 2003; but see Chao et al., 1999). Adam and Noppeney (2010), using visual stimuli, localized VTC regions showing animal (fusiform gyrus) or place (PPA) selectivity and then measured responses to animal and place sounds, such as “meow” for cat. They found that the PPA was selective for land-

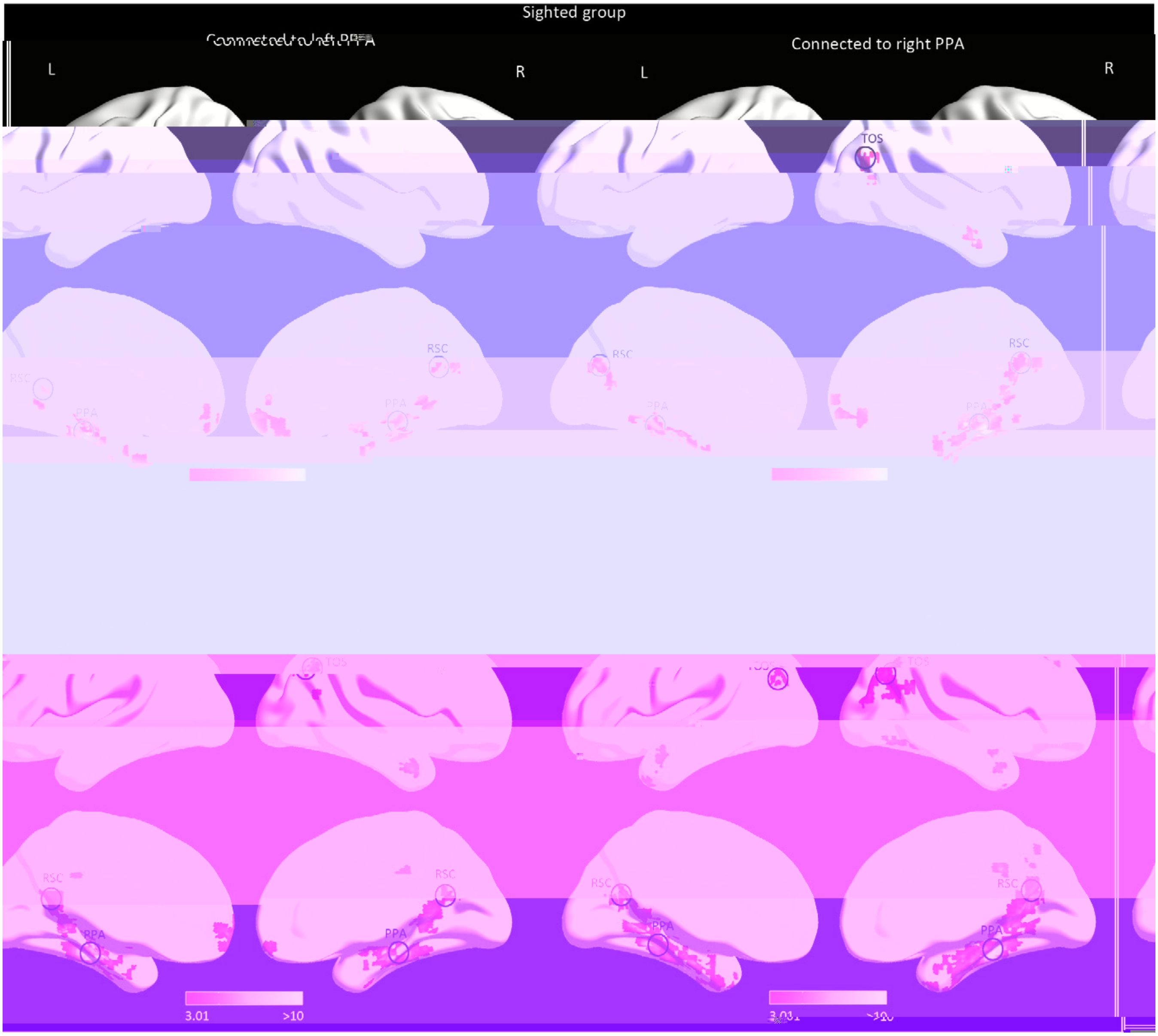

Fig. 3. Functional connectivity of the resting-state data. For the sighted group, the seed regions (bilateral PPA) were defined by the conjunction of large nonmanipulable object > tool & large nonmanipulable object > animal in sighted group's auditory experiment. For the blind participants, the seed regions (bilateral PPA) were defined by the conjunction of large nonmanipulable object > tool & large nonmanipulable object > animal in blind group's auditory experiment. The whole-brain functional connectivity with the seed regions was calculated voxel by voxel ($p < .05$ AlphaSim corrected). Voxels showing significant positive functional connectivity with the seed regions are shown on the red–yellow color scale.

specific content of the representations in the visual cortex of congenitally blind individuals is different from that in sighted individuals (e.g., visual imagery), it is more parsimonious to assume that at least part of the organization of higher-level visual cortex is independent of visual experience (Mahon and Caramazza, 2011).

Finally, the similar resting-state functional connectivity patterns associated with PPA in the sighted and the blind groups provide new insights into the potential mechanisms for PPA's functional profile. While accumulating evidence has shown that scene or navigation related tasks co-activate PPA, RSC and TOS (e.g., Epstein, 2008), which is commonly referred to as the “scene network”, our study shows for the first time that PPA is intrinsically connected with RSC and TOS even in the absence of any explicit task requirements. The finding that this intrinsic network is independent of visual experience, in association with the similar functional selectivity for large nonmanipulable objects in these regions, is in line with the theoretical proposal that the categorical organization within VTC is partly driven by differential connectivity with other functionally relevant brain regions (Mahon and Caramazza, 2011; Mahon et al., 2007). The exact role of these intrinsic connections in object processing and whether these connections are modulated by specific tasks differently in sighted and blind participants warrant further investigation.

To conclude, we observed selectivity for large nonmanipulable objects relative to animals and tools in PPA in both sighted (picture viewing and auditory) and congenitally blind participants (auditory), with similar patterns also observed in two additional scene-selective regions in TOS and RSC. These regions are intrinsically connected with each other, in both blind and sighted groups, and may be sensitive to information related to navigation that is independent of visual experience. More generally, the highly similar categorical organization in individuals with and without visual experience, when performing identical task, suggests that the large-scale organization of high-order visual cortex may not be primarily shaped by visual input.

Funding

This work was supported by the 973 Program (2013CB837300), the NSFC (31171073; 31222024; 31271115), and the Fondazione Cassa di Risparmio di Trento e Rovereto.

Supplementary data to this article can be found online at http://dx.doi.org/10.1016/j.neuroimage.2013.04.051.

Acknowledgments

We thank Xueming Lu for his assistance in data analyses, and all BNU-CNLab members for their aids in data collection.

Conflict of interest statement

No author has any conflict of interest with respect to this article.

References

Adam, R., Noppeney, U., 2010. Prior auditory information shapes visual category-selectivity in ventral occipito-temporal cortex. NeuroImage 52, 1592–1602.

Amedi, A., Floel, A., Knecht, S., Zohary, E., Cohen, L.G., 2004. Transcranial magnetic stimulation of the occipital pole interferes with verbal processing in blind subjects. Nat. Neurosci. 7, 1266–1270.

Bar, M., 2004. Visual objects in context. Nat. Rev. Neurosci. 5, 617–629.

Bar, M., Aminoff, E., 2003. Cortical analysis of visual context. Neuron 38, 347–358.

Bracci, S., Ietswaart, M., Peelen, M.V., Cavina-Pratesi, C., 2010. Dissociable neural responses to hands and non-hand body parts in human left extrastriate visual cortex. J. Neurophysiol. 103, 3389–3397.

Bracci, S., Cavina-Pratesi, C., Ietswaart, M., Caramazza, A., Peelen, M.V., 2012. Closely overlapping responses to tools and hands in left lateral occipitotemporal cortex. J. Neurophysiol. 107, 1443–1456.

Chao, L.L., Haxby, J.V., Martin, A., 1999. Attribute-based neural substrates in temporal cortex for perceiving and knowing about objects. Nat. Neurosci. 2, 913–919.

Cohen, L., Dehaene, S., 2004. Specialization within the ventral stream: the case for the visual word form area. NeuroImage 22, 466–476.

Collignon, O., Vandewalle, G., Voss, P., Albouy, G., Charbonneau, G., Lassonde, M., Lepore, F., 2011. Functional specialization for auditory–spatial processing in the occipital cortex of congenitally blind humans. Proc. Natl. Acad. Sci. U. S. A. 108, 4435–4440.

Devlin, J.T., Rushworth, M.F.S., Matthews, P.M., 2005. Category-related activation for written words in the posterior fusiform is task specific. Neuropsychologia 43, 69–74.

Downing, P.E., Jiang, Y., Shuman, M., Kanwisher, N., 2001. A cortical area selective for visual processing of the human body. Science 293, 2470–2473.

Downing, P.E., Chan, A.W., Peelen, M.V., Dodds, C.M., Kanwisher, N., 2006. Domain specificity in visual cortex. Cereb. Cortex 16, 1453–1461.

Epstein, R.A., 2008. Parahippocampal and retrosplenial contributions to human spatial navigation. Trends Cogn. Sci. 12, 388–396.

Epstein, R.A., Kanwisher, N., 1998. A cortical representation of the local visual environment. Nature 392, 598–601.

Epstein, R.A., Ward, E.J., 2010. How reliable are visual context effects in the parahippocampal place area? Cereb. Cortex 20, 294–303.

Epstein, R.A., Harris, A., Stanley, D., Kanwisher, N., 1999. The parahippocampal place area: recognition, navigation, or encoding? Neuron 23, 115–125.

Epstein, R.A., Higgins, J.S., Jablonski, K., Feiler, A.M., 2007. Visual scene processing in familiar and unfamiliar environments. J. Neurophysiol. 97, 3670–3683.

Goh, J.O.S., Siong, S.C., Park, D., Gutchess, A., Hebrank, A., Chee, M.W.L., 2004. Cortical areas involved in object, background, and object-background processing revealed with functional magnetic resonance adaptation. J. Neurosci. 24 (45), 10223–10228.